Additive Manufacturing 8 (2015) 63–70

Contents lists available at ScienceDirect

Additive Manufacturing

journal homepage: www.elsevier.com/locate/addma

Electron beam welding of AlSi10Mg workpieces produced by selected laser melting additive manufacturing technology

Moshe Nahmany[a,*], Idan Rosenthal[b], Isgav Benishti[a], Nachum Frage[b], Adin Stern[b]

[a] Materials Department, Nuclear Research Center, Negev, P.O.B. 9001, Beer Sheva 8410900, Israel
[b] Materials Engineering Department, Ben Gurion University of the Negev, P.O.B. 653, Beer Sheva 8410501, Israel

ARTICLE INFO

Article history:
Received 11 February 2015
Received in revised form 20 June 2015
Accepted 24 August 2015
Available online 28 August 2015

Keywords:
AM
SLM
AlSi10Mg alloy
EBW

ABSTRACT

Electron beam welding (EBW) is a high-density energy (low heat input) welding technique, resulting in a narrow heat affected zone (HAZ), causing minimal metallurgical changes in the workpieces. The present research work investigates EB autogenous welded AlSi10Mg samples, produced by the selective laser melting (SLM) additive manufacturing (AM) method, with emphasis on the characterization of the joint's macro- and microstructure. When comparing the EB welded AM parts to the EB welded cast samples two main differences were observed: weld metal porosity and a negligible HAZ in the AM joints and low porosity level but substantial HAZ in the welded cast parts. These preliminary results show for the first time the feasibility of the EBW technique on AM-SLM specimens.

1. Introduction

The concept of advanced manufacturing technology has been viewed as the utilization of computer and numerical-based processing of components. One of these technologies includes three-dimensional printing and related layer-by-layer fabrication, known as additive manufacturing (AM) [1–4]. AM technology builds a solid, often geometrically complex object from a series of layers, each one "printed" on top of the previous one. AM "printers" use a virtual, mathematical model to construct a physical artifact that can be manipulated on the computer screen. Manufacturing components (by powder-bed process, for example) offers a high geometrical flexibility and accuracy enabling the construction of components with very complex external and internal shapes (e.g. embedded cooling channels). The AlSi10Mg alloy, which was investigated in the present study, is a widely used casting alloy with near-eutectic composition, displaying good mechanical properties and weldability. The addition of small amounts of Mg (0.3–0.5 wt.%) provides precipitation hardening of the aluminum alloy by forming Mg_2Si precipitates upon natural or artificial aging treatments [5]. Typical hardness values of AlSi10Mg fabricated by AM-SLM are reported [6] as 94 ± 5 HV and up to 120 ± 5 HV (reported [7] as 120 ± 5 HBW). The engineering design of many structural components requires the manufacturing of complex shaped modules which is quite expensive. An attractive way to achieve this goal is to fabricate the composite modules by joining two or more AM processed components. A reliable joining technology provides enhanced design flexibility and engineering solutions for AM modules that are impossible to produce due to size limitations of the additive manufacturing equipment.

Power beam welding processes characterized by energy densities up to 10^6 W/cm^2 [8], are ideally suited for producing high quality welds, both minimizing the weld heat input and reducing the weld-induced distortion of the components. The EBW process (Fig. 1a) has been chosen in this research because it is well-positioned to provide metal industries with high quality and reliable joining solutions.

Moreover, the solidification rates for this process (10^5–10^6 °C/s) are significantly higher than those for conventional arc welding processes (10^2–10^3 °C/s), creating the fine microstructure of the weld metal. There are four major types of weld defects in EBW of aluminum: porosity, cracking, inclusions and loss of alloying elements [9]. The porosity is usually located in the keyhole path, whereas gas pores are homogeneously distributed with slight enrichment at the melting line. When the welding mode switches from the keyhole to conduction mode, the level of porosity is significantly reduced, because there is enough time for gases to escape from a shallower weld pool.

2. Goals of research

- Demonstrate the feasibility of using EBW technology to weld SLM AlSi10Mg components.

* Corresponding author.
E-mail address: moshesig@gmail.com (M. Nahmany).

http://dx.doi.org/10.1016/j.addma.2015.08.002
2214-8604/

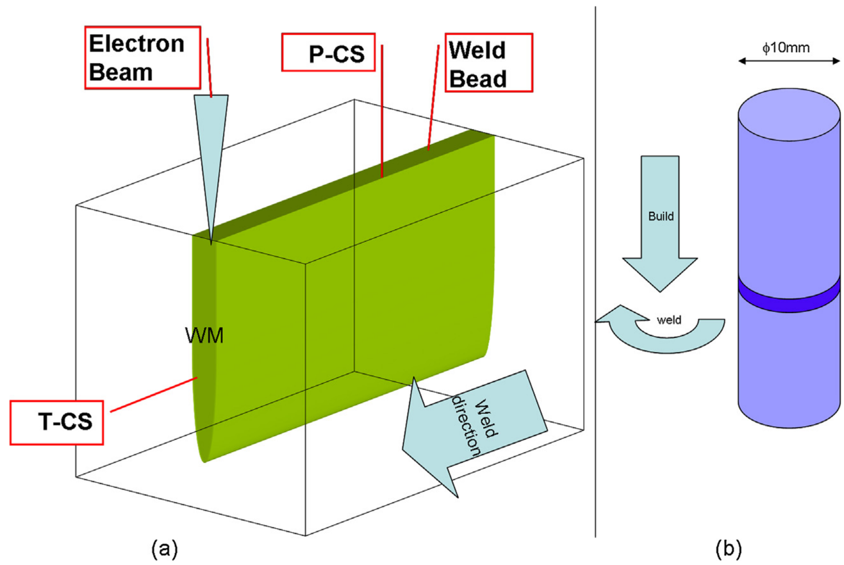

Fig. 1. (a) Schematic illustration of the EBW process, presenting a deep and narrow weld metal (WM). The illustration displays the metallographic cross sections: T-CS for transverse, P-CS for planar. (b) Schematic illustration of the welded specimens, presenting the build direction and the weld direction.

- Compare the microstructure of EBW joined region of SLM-produced specimens and casting-produced specimens.

3. Experimental

Welding samples were machined from AM-SLM built AlSi10Mg commercial specimens, manufactured using an EOSINT-M280 system. Pre-alloyed AlSi10Mg powder with particle size distribution between 7 and 50 μm has been used [10]. All specimens were built in the vertical direction. The welding samples were machined from 10 mm diameter rods and axially aligned for the welding operation. The circumferential welds were oriented perpendicularly to the building direction (Fig. 1b). For the sake of comparison, welding specimens were prepared from A356-T6 plates fabricated by casting. Autogenous electron beam welding technique was used to join both types of specimens on a Wentgate EB machine with capabilities of 60 kV acceleration voltage and a 40 mA beam current. The machine is equipped with both rotational turntable and XY-stage. The electron beam can be consistently focused (with diameter about 0.3–0.5 mm) on the specimen's top surface for all welds. Welds were performed with electron beam power varying from 120 to 600 W using heat inputs of 21–45 J/mm. Welding parameters are presented in Table 1. Welding parameters were selected using our experience on EBW of cast aluminum and were updated according to the preliminary results of EBW of AM parts. We have tried to keep some parameters constant and vary others to clarify their effects.

The joints were characterized to visualize the development of novel and unusual macrostructures and microstructural architectures resulting from EB welding of the AlSi10Mg alloy. Welds were characterized from a transverse cross-section and from a planar cross-section noted as T-CS and P-CS respectively. Metallographic samples were prepared according to the ASTM-E3 Standard. First, the samples were hot mounted, and then a rough polish was performed. Surface preparation was performed by grinding and fine polishing (up to 0.5 μm) and etched in Flick's Reagent (10% HF–90% H_2O) to expose the microstructure. Welds were examined by an Optical Microscope (OM Zeiss, Aalen, Germany), Scanning Electron Microscope (SEM JEOL, JSM-2500) and High Resolution Scanning Electron Microscope (HRSEM, JEOL 7400F). Micro-hardness tests were conducted using a Buehler micro-hardness tester (MMT-7), with a load of 100 g.

Table 1
Welding parameters; all welds were performed using 60 kV acceleration voltage. Last specimens, designated with "C" are cast specimens. Heat input was calculated as (beam current × beam voltage)/welding speed.

No.	Travel speed (mm/min)	Beam current (mA)	Heat input/specific energy (J/mm)
1	1000	6	21.7
2	1000	8	28.8
3	1000	10	36
4	1000	13	46.8
5	750	6	28.8
6	500	4	28.8
7	484	4	29.8
8	242	2	29.8
9	484	3	22.3
10	242	3	44.7
11	1000	8	28.8
12	500	4	28.8
C-13	1000	5.5	19.9
C-14	1000	16	57.6

4. Results and discussion

4.1. Base metal composition and microstructure

The microstructure of the components fabricated by the AM is the end-result of pre-alloyed powder melting/solidification, with adjacent neighboring tracks responsible for partial remelting of the solidified tracks. Average concentrations (in wt.%) of the alloying elements are 11.1 Si, 0.2 Mg, ~0.1 Fe with traces of Cr, Cu, Mn, Ti, and Zn. the concentration of the alloying elements in the base metal was determined by a wet chemical analysis. The typical microstructure of the AlSi10Mg part (Fig. 2a and b), consisting of approximately half-cylindrical solidified melt pools, reveals that most of the defects (Fig. 2c) are located at regions where the melt pools overlap, strengthening the role of the melting/solidification cycles and their effect on both microstructure and defect formation. The fast melting process of the stochastic powder bed can induce vigorous melt pool movements which sometimes lead to faults acting as starting points for defects such as channels and/or pores between layers [6,10,11]. The microstructure morphology is